nature cell biology

Tudor staphylococcal nuclease is an evolutionarily conserved component of the programmed cell death degradome

Jens F. Sundström[1,9], Alena Vaculova[2,9], Andrei P. Smertenko[3,9,10], Eugene I. Savenkov[1,9], Anna Golovko[1,9], Elena Minina[1,9], Budhi S. Tiwari[1], Salvador Rodriguez-Nieto[2], Andrey A. Zamyatnin Jr[1], Tuuli Välineva[4], Juha Saarikettu[4], Mikko J. Frilander[5], Maria F. Suarez[6], Anton Zavialov[7], Ulf Ståhl[1], Patrick J. Hussey[3], Olli Silvennoinen[4,8], Eva Sundberg[1], Boris Zhivotovsky[2] and Peter V. Bozhkov[1,10]

Programmed cell death (PCD) is executed by proteases, which cleave diverse proteins thus modulating their biochemical and cellular functions. Proteases of the caspase family and hundreds of caspase substrates constitute a major part of the PCD degradome in animals[1,2]. Plants lack close homologues of caspases, but instead possess an ancestral family of cysteine proteases, metacaspases[3,4]. Although metacaspases are essential for PCD[5–7], their natural substrates remain unknown[4,8]. Here we show that metacaspase mcII-Pa cleaves a phylogenetically conserved protein, TSN (Tudor staphylococcal nuclease), during both developmental and stress-induced PCD. TSN knockdown leads to activation of ectopic cell death during reproduction, impairing plant fertility. Surprisingly, human TSN (also known as p100 or SND1), a multifunctional regulator of gene expression[9–15], is cleaved by caspase-3 during apoptosis. This cleavage impairs the ability of TSN to activate mRNA splicing, inhibits its ribonuclease activity and is important for the execution of apoptosis. Our results establish TSN as the first biological substrate of metacaspase and demonstrate that despite the divergence of plants and animals from a common ancestor about one billion years ago and their use of distinct PCD pathways, both have retained a common mechanism to compromise cell viability through the cleavage of the same substrate, TSN.

Gene expression is controlled by specialized sets of proteins functioning through several pathways at transcriptional and post-transcriptional levels. One of these proteins, TSN, functions in activating transcription[9,10,13], subsequent mRNA splicing[15], regulation of RNA silencing (as a component of the RNA-induced silencing complex, RISC)[11] and in the pathway that edits and destroys double-stranded RNA[12,14]. The ability of TSN to perform several functions is attributed to its complex domain structure. TSN is composed of a single Tudor domain and five staphylococcal nuclease (SN)-like domains (Fig. 1a; Supplementary Information, Fig. S1)[16]. Sequence analysis of *Homo sapiens* TSN (HsTSN) protein revealed a DAVD 790 motif, a known consensus cleavage site for caspase-3-like enzymes[17,18], between the Tudor and the fifth SN (SN5) domains (Fig. 1a; Supplementary Information, Fig. S1). Correspondingly, caspase-3 processed recombinant HsTSN into large (relative molecular mass of about 90,000, M_r 90K) and small (about 10K) fragments, and inhibition of caspase-3 with DEVD-CHO abolished the cleavage (Fig. 1b). Amino-terminal sequencing of the fragments confirmed the predicted cleavage of HsTSN after the DAVD 790 motif.

Induction of apoptosis in HCT116 colon carcinoma cells with 5-fluorouracil (5FU) led to increased caspase-3-like activity and cleavage of endogenous HsTSN into two fragments with the same molecular mass, as observed *in vitro* (Fig. 1b, c). This effect was not cell- and drug-specific because a similar pattern of endogenous HsTSN cleavage was detected in camptothecin (CPT)-treated HeLa cells (Fig. 1d). As the proteolysis of HsTSN did not occur either when the P1 position of the DAVD motif was mutated (TSN^{D790E}) or after treatment with the pan-caspase inhibitor zVAD-fluoromethylketone (zVAD-fmk; Fig. 1d, e), we conclude that HsTSN is a new component of the human PCD degradome and is cleaved by caspase-3 between the Tudor and SN5 domains.

Next, the physiological significance of HsTSN proteolysis was examined using cells transfected with non-cleavable TSN^{D790E}. Expression of

[1]Department of Plant Biology and Forest Genetics, Uppsala BioCenter, Swedish University of Agricultural Sciences, Box 7080, SE-75007 Uppsala, Sweden. [2]Institute of Environmental Medicine, Karolinska Institutet, Box 210, SE-17177, Stockholm, Sweden. [3]The Integrative Cell Biology Laboratory, School of Biological and Biomedical Sciences, University of Durham, South Road, Durham DH1 3LE, UK. [4]Institute of Medical Technology, University of Tampere, FIN-33014 Tampere, Finland. [5]Institute of Biotechnology, University of Helsinki, FIN-00014 Helsinki, Finland. [6]Departamento de Biologia Molecular y Bioquimica, Facultad de Ciencias, Universidad de Malaga, Campus de Teatinos, 29071 Malaga, Spain. [7]Department of Molecular Biology, Biomedical Center, Swedish University of Agricultural Sciences, Box 590, SE-75124 Uppsala, Sweden. [8]Department of Clinical Microbiology, Tampere University Hospital, FIN-33520 Tampere, Finland.
[9]These authors contributed equally to this work.
[10]Correspondence should be addressed to P.V.B. or A.P.S (e-mails: peter.bozhkov@vbsg.slu.se; andrei.smertenko@durham.ac.uk).

Received 26 May 2009; accepted 3 August 2009; published online 11 October 2009; DOI: 10.1038/ncb1979

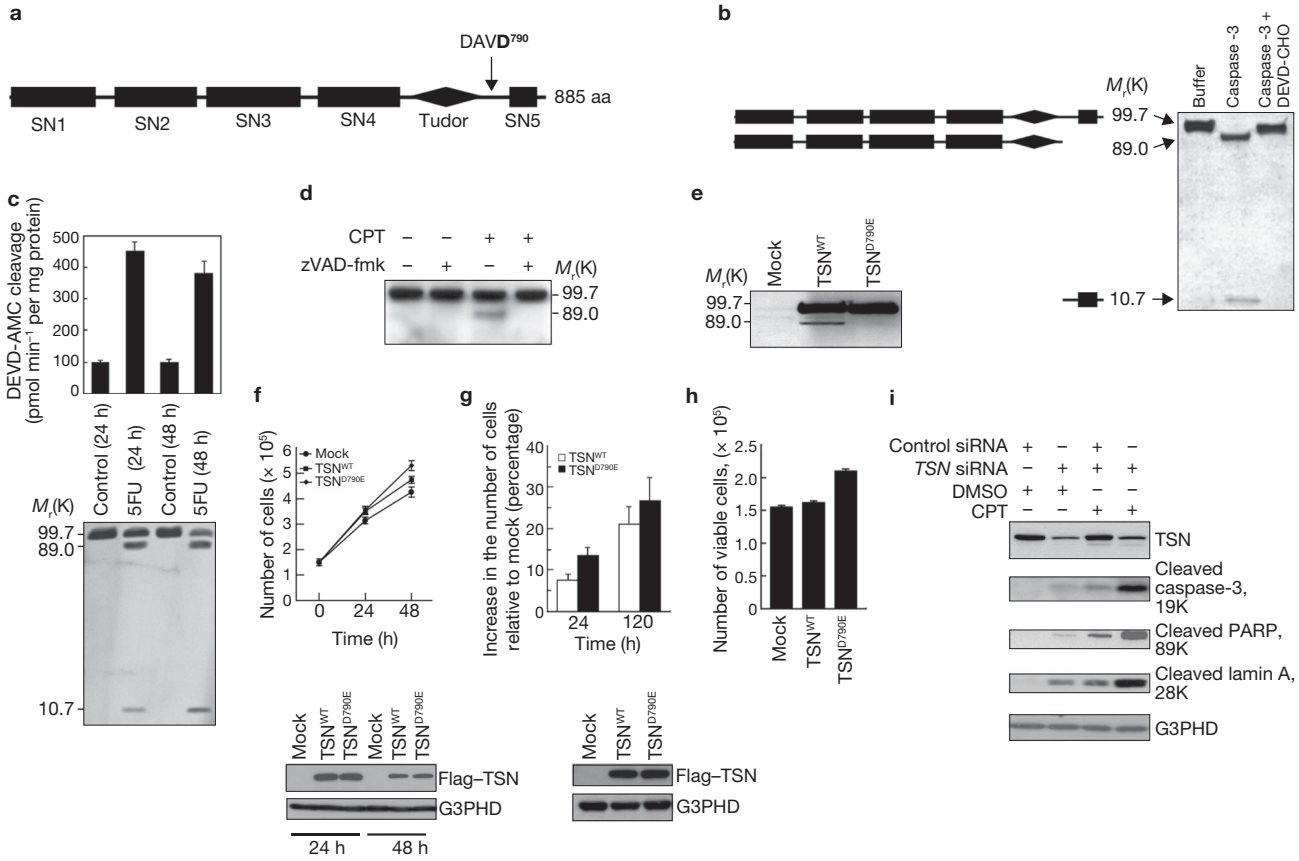

Figure 1 Human TSN is a substrate for caspase-3 and is essential for cell viability. (**a**) Domain structure of HsTSN. The caspase cleavage motif DAVD is situated between the Tudor and SN5 domains. (**b**) Cleavage of HsTSN by caspase-3 *in vitro*. Recombinant HsTSN was incubated alone (buffer), with caspase-3, or with caspase-3 and DEVD-CHO. The reactions were separated on SDS–PAGE and stained with Coomassie blue. Molecular masses and identities of HsTSN fragments (left) were obtained by peptide sequencing. (**c**) Treatment of HCT116 cells with 5FU (50 μg ml^{-1}) stimulates caspase-3-like activity (graph) and induces fragmentation of endogenous HsTSN (western blot with anti-TSN). (**d**) zVAD-fmk prevents HsTSN fragmentation. Western blot, using an anti-TSN antibody, of HeLa cell protein extracts from control cells and cells treated for 24 h with CPT (5 μM) and/or zVAD-fmk (15 μM). (**e**) Mutation of Asp 790 abolishes HsTSN cleavage. Western blot, using an anti-Flag antibody, of protein extracts from HeLa cells transfected with an empty vector (Mock), wild-type TSN or TSN^{D790E} and treated for 24 h with CPT (5 μM). HsTSN was Flag-tagged at its N-terminal. (**f, g**) Expression of TSN^{D790E} promotes cell proliferation. (**f**) Total number of HeLa cells in cultures transfected with the indicated constructs. Only TSN^{D790E} samples showed significant increase in cell proliferation 48 h after transfection (Tukey test; $P < 0.05$; versus mock). Western blot with anti-Flag shows equal amounts of exogenous HsTSN in transfected cells. (**g**) There was an increase in the number of HEK293 cells after transfection with wild-type TSN or TSN^{D790E} relative to mock. Proliferation in TSN^{D790E} samples was twofold higher after 24 h (Tukey test; $P < 0.05$; versus wild-type TSN). Western blot shows equal amount of exogenous HsTSN 24 h after transfection. (**h**) Expression of TSN^{D790E} attenuates cell death. The graph shows the number of attached viable HeLa cells transfected with the indicated constructs after 24 h of treatment with CPT (5 μM). (**i**) Downregulation of HsTSN promotes apoptosis. Western blots with anti-TSN and antibodies against cleaved forms of caspase-3, PARP and lamin A using protein extracts from HeLa cells transfected with control or *TSN* siRNA for 48 h and then treated with CPT (7.5 μM) or DMSO (vehicle), for 5 h. Molecular weights are presented as relative molecular mass, M_r(K). Data in **c**, **f**, **g** and **h** represent the mean ± s.e.m. from three (**c**) or four (**f**, **g** and **h**) independent experiments. G3PDH is a loading control. Full scans of blots in **b**–**e** and **i** are shown in Supplementary Information, Fig. S7. WT, wild type.

TSN^{D790E} under normal conditions enhanced cell proliferation in both cancer (HeLa) and non-cancer (HEK293) cells compared with mock- and wild-type HsTSN-transfected samples (Fig. 1f, g). Under CPT-induced apoptosis, expression of TSN^{D790E} resulted in a 35% increment in viable HeLa cells (Fig. 1h), suggesting that caspase-mediated proteolysis of HsTSN is important for the progression of apoptosis.

As uncleavable TSN stimulates cell proliferation and protects cells from death, we proposed that a reduction in TSN levels should render cells more susceptible to the induction of apoptosis. Indeed, HeLa cells transfected with *TSN* short interfering RNA (siRNA) showed a dramatic increase in apoptotic response to CPT (Fig. 1i) accompanied by a 7.9 ± 2.9-fold increase in activation of caspase-3 and increased cleavage of PARP and lamin-A (by 3.7 ± 0.5-fold and 6.7 ± 2.9-fold, respectively) as measured by densitometry ($n = 3$). Moreover, reduction of TSN levels induced apoptosis even in the absence of CPT, leading to 7.7 ± 1.9-fold, 6.1 ± 1.3-fold and 11 ± 1.9-fold increases in apoptotic markers (Fig. 1i), demonstrating that HsTSN is indispensable for the maintenance of cell viability.

Although TSN is an evolutionarily conserved protein (Supplementary Information, Fig. S2a), the DAVD caspase-3 cleavage motif is only conserved in vertebrate TSN homologues and is absent from protozoa, fungi and plants (Supplementary Information, Fig. S2b). These organisms do not have close homologues of caspases, but possess a family of distantly related cysteine proteases, metacaspases, which share a caspase-specific catalytic diad of histidine and cysteine as well as a caspase-like secondary structure[3,4]. Although metacaspases lack aspartate specificity, cleaving

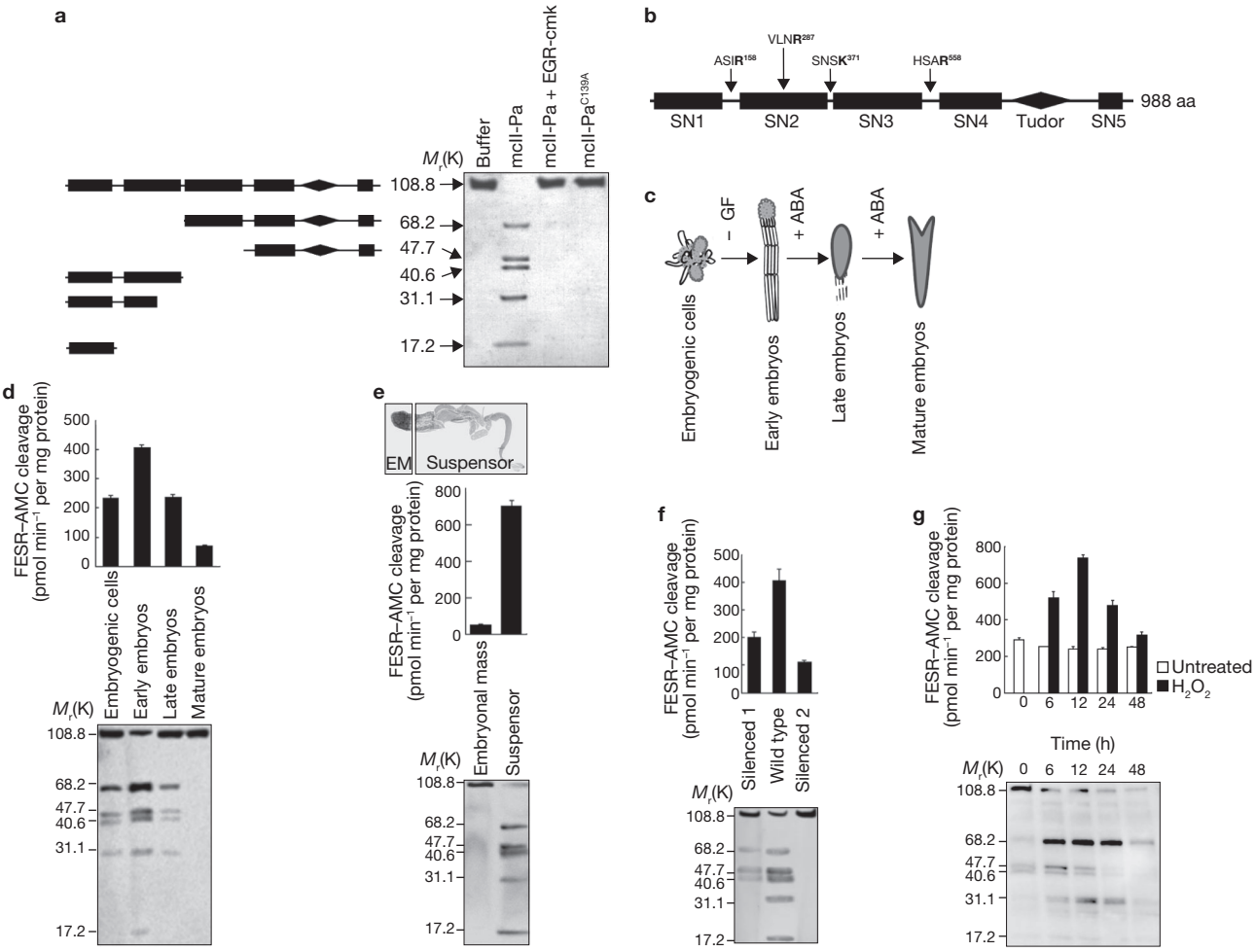

Figure 2 Plant TSN is a substrate for metacaspase during developmental and stress-induced cell death. (**a**) PaTSN is cleaved by metacaspase mcII-Pa *in vitro*. Recombinant PaTSN was incubated alone (buffer), with wild-type recombinant mcII-Pa, wild-type mcII-Pa and its inhibitor EGR-cmk, or with a catalytically inactive mcII-Pa mutant (mcII-Pa^{C139A}). The reactions were separated on SDS–PAGE and stained with Coomassie blue. Molecular masses and identities of PaTSN fragments (left) were obtained from peptide sequencing. (**b**) Domain organization of PaTSN and location of mcII-Pa cleavage sites. (**c**) A schematic model of highly stereotyped and synchronized pathway of somatic embryo development in *P. abies*. The proliferation of embryogenic cells is stimulated by growth factors (GF; auxin and cytokinin). The development of early embryos is induced by withdrawal of GF. Early embryos are composed of living embryonal masses (apical) and dying suspensors (basal). Late embryogeny and embryo maturation are promoted by abscisic acid (ABA). The embryo-suspensors are eliminated during late embryogeny. (**d–f**) Cleavage of endogenous PaTSN (western blots) correlates with metacaspase activity (graphs). (**d**) Samples were collected 7 days after addition of GF (embryogenic cells), 7 days after withdrawal of GF (early embryos), and 7 days (late embryos) and 35 days (mature embryos) after addition of ABA. (**e**) Samples from microsurgically separated embryonal masses (EM) and suspensors collected 7 days after withdrawal of GF (depicted on the micrograph). (**f**) Samples from a wild-type cell line and two *mcII-Pa* RNAi-silenced clones, 7 days after withdrawal of GF. (**g**) Cleavage of endogenous PaTSN (western blot) and metacaspase activity (graph) during stress-induced cell death. Hydrogen peroxide and GF were added simultaneously, and samples were collected after 0, 6, 12, 24 and 48 h. The metacaspase activity was measured using AMC-conjugated FESR peptide[6]. Data represent the mean ± s.e.m from three independent experiments. Full scans of the gel in **a** and blots in **d–g** are shown in Supplementary Information, Fig. S7.

synthetic peptides after arginine and lysine residues[6,19–21], they have been suggested to be functional homologues of caspases[6,22,23].

Plant metacaspases are involved in the regulation of both developmental PCD during embryogenesis[5,6] and abiotic stress-induced PCD[7]. We have previously reported that the activation of metacaspase mcII-Pa from Norway spruce (*Picea abies*) requires autoprocessing of the zymogen at two sites, FESR 188 and KFVK 269 (ref. 6). Therefore, plant TSN sequences were analysed for the presence of metacaspase cleavage sites, with consideration given to the facts that (i) autoprocessing sites of the proteases can mimic cleavage sites of their substrates[24] and (ii) *Arabidopsis thaliana* metacaspase AtMC9 has a higher preference for cleavage sites with a large aliphatic or aromatic residue at the P4 position[21]. All plant TSN proteins were found to contain several metacaspase cleavage sites, indicating that plant TSN might be a substrate for metacaspases.

To address this hypothesis, we cloned a full-length cDNA from *P. abies* encoding TSN (PaTSN; Supplementary Information, Fig. S1) and produced recombinant protein. Metacaspase mcII-Pa processed recombinant PaTSN into five major fragments (Fig. 2a). Inactivation of mcII-Pa either by the inhibitor EGR-chloromethyl ketone (EGR-cmk) or through mutation of catalytic Cys 139 (ref. 6) blocked TSN fragmentation (Fig. 2a). Sequencing of PaTSN fragments identified at least four cleavage sites, all but one located between SN domains, with either arginine or lysine at the P1 position (Fig. 2b).

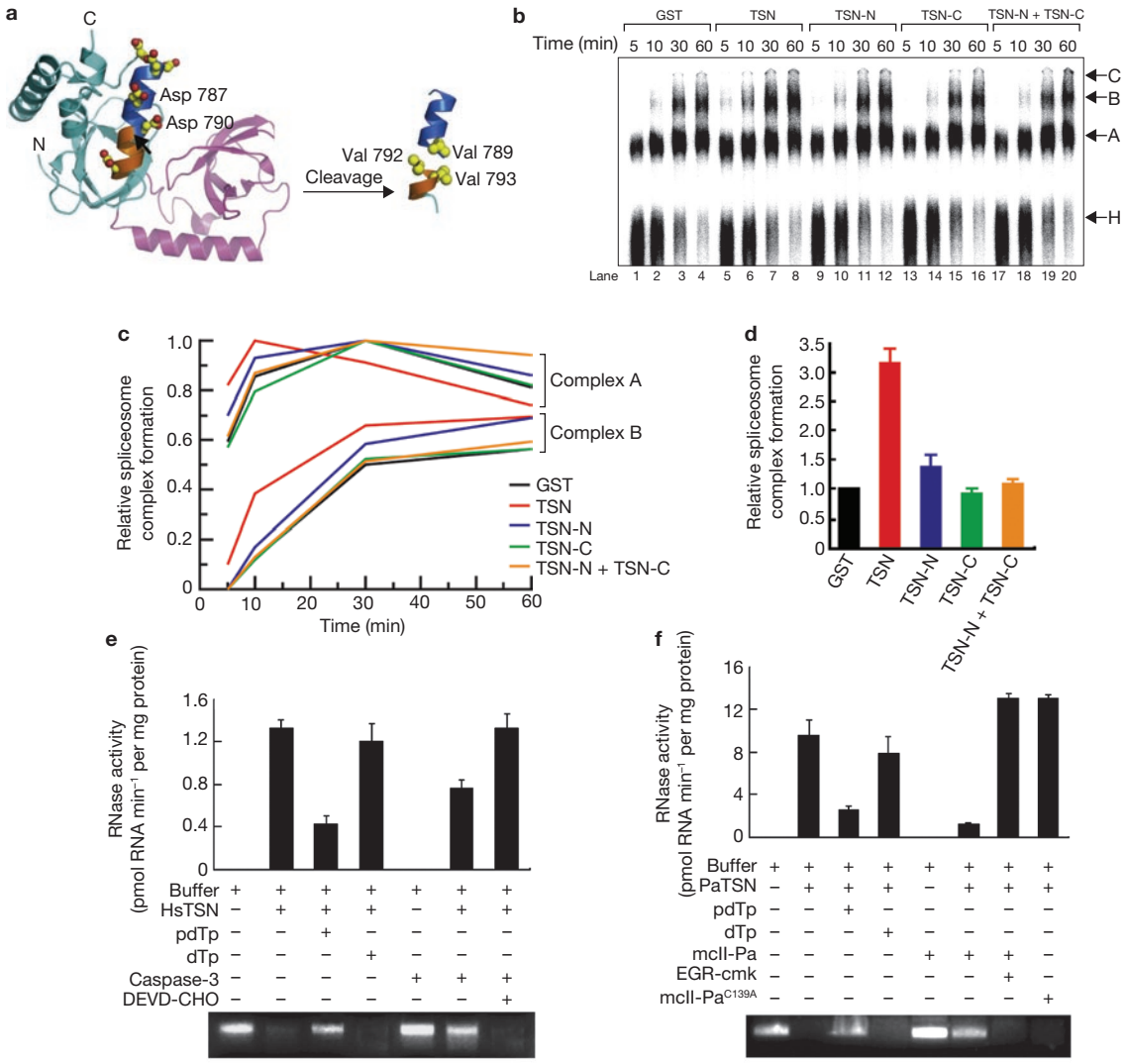

Figure 3 Proteolytic cleavage inhibits TSN function. (**a**) Diagram illustrating cleavage of HsTSN by caspase-3. Cyan, SN5 domain; pink, Tudor domain. The caspase-3 cleavage motif is located within the α2 helix (marine from Asp 781 to Asp 790 and orange from Ser 791 to Gln 797). The α2 helix exposes six Asp residues, creating a highly negatively charged patch on the surface of the SN5 domain, potentially facilitating recognition of the DAVD motif by caspase-3. Cleavage between Asp 790 and Ser 791 (short black arrow) splits the helix into two smaller helices (blue and orange). Collisions between the C-terminal carboxyl and N-terminal amino groups introduce a gap in the new structure and cause three Val residues, 789, 792 and 793, to associate with a surface-exposed hydrophobic cluster. Side chains of aspartate and valine residues are shown as spheres and are coloured by type of element: carbon, yellow; oxygen, red. (**b**–**d**) Truncated TSN is unable to stimulate spliceosome complex formation. (**b**) Autoradiogram of native gel analysis of spliceosome assembly reactions supplemented with GST (negative control, lanes 1–4), full-length mouse TSN (lanes 5–8), N-terminal fragment of TSN (lanes 9–12), C-terminal fragment of TSN (lanes 13–16) or a mixture of N- and C-terminal fragments (lanes 17–20). The bands corresponding to the non-specific complex H, and spliceosomal complexes A, B and C are indicated on the right. The C-complex band is diffuse and does not separate well on this gel. **(c)** Quantitative analysis of spliceosomal complex formation. The quantification was performed using phosphorimager and the results were normalized by setting the highest complex A value observed within each time series to one. (**d**) Comparison of complex B formation at 10 min. Data were normalized by setting the value of reactions containing GST to one and they represent the mean ± s.e.m. from three independent experiments. (**e**, **f**) Proteolytic cleavage inhibits nucleolytic activity of TSN. Recombinant HsTSN (**e**) and PaTSN (**f**) were incubated in buffer containing additional components as indicated in the figure, and then RNA substrates were added and ribonuclease activity determined by electrophoretic (gels) or fluorometric (graphs) assays. Data on the graphs represent the mean ± s.e.m. from three independent experiments.

PCD is paramount for plant embryogenesis, particularly for the elimination of a terminally differentiated temporary organ, the embryo suspensor[25,26]. Metacaspase mcII-Pa is a key executioner of this PCD, taking part in nuclear disassembly[6]; silencing of *mcII-Pa* suppresses PCD and blocks embryonic pattern formation[5]. The *P. abies* embryogenesis model system[25,26] (Fig. 2c) has been used for functional analysis of PaTSN during PCD. The proteolytic activity of mcII-Pa was measured at four successive stages of embryogenesis using the peptidic substrate FESR-AMC and was compared with the PaTSN fragmentation pattern. Metacaspase activity correlated with accumulation of the processed form of mcII-Pa and the proportion of cells undergoing PCD (Supplementary Information, Fig. S3a–c). Whereas the highest activity was detected in the early embryos composed of living embryonal masses and dying embryo-suspensors, the lowest activity was found in the mature embryos,

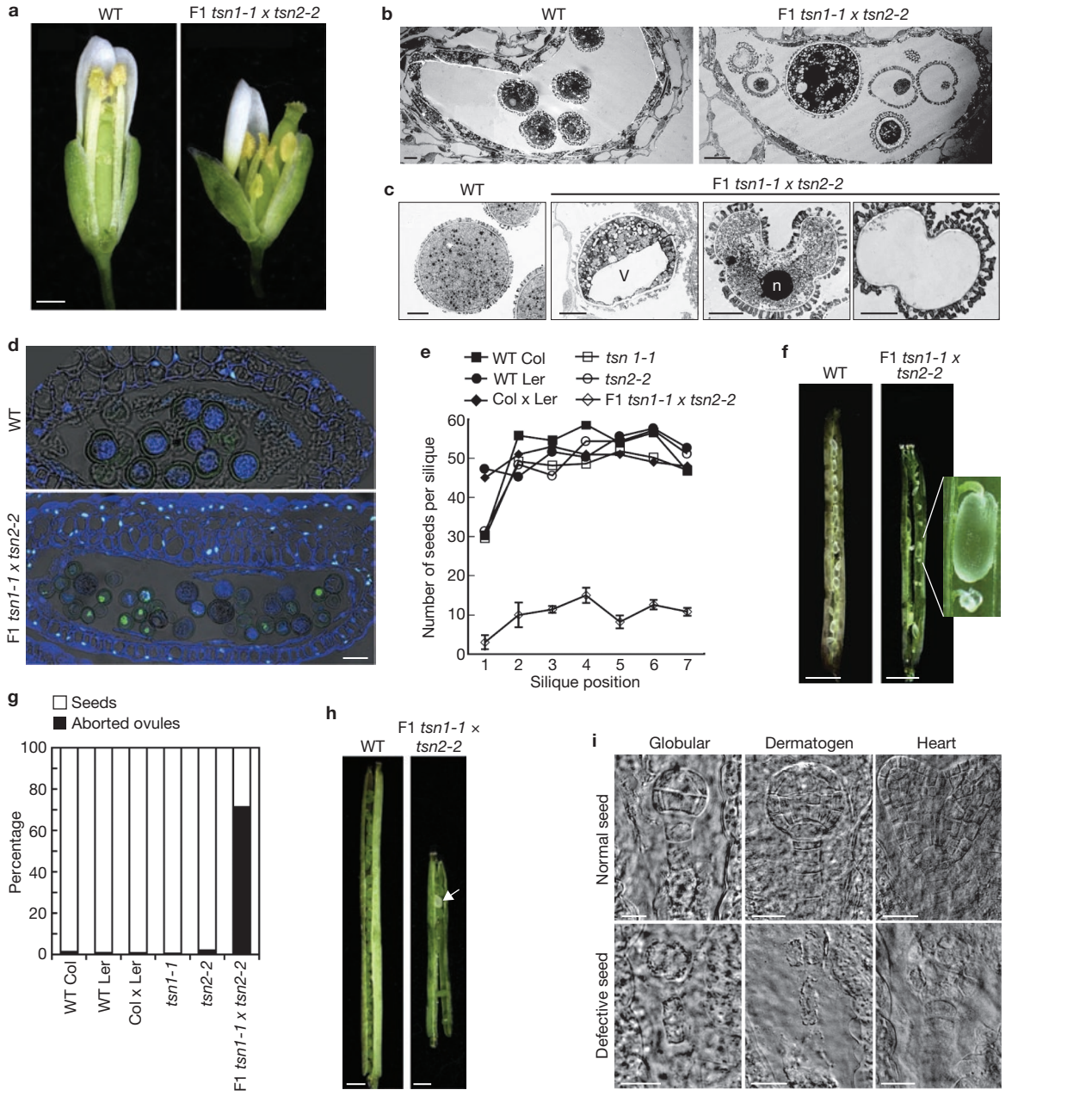

Figure 4 TSN proteins are important for *Arabidopsis* pollen development and embryogenesis. (**a**) Morphology of wild-type and F1-generation flowers. Note short stamens in F1 flowers. Scale bar, 0.5 mm. (**b**, **c**) Electron micrographs of anther locules (**b**) and individual pollen grains (**c**) in wild-type and F1 stage-11 flowers. Most F1 pollen grains contain large vacuoles (v), condensed nuclei (n) and in some cases no cytoplasm. Scale bars, 5 μm in **b** and 2.5 μm in **c**. (**d**) *In situ* detection of DNA fragmentation (TUNEL; green) in anthers; the samples were counterstained with DAPI (4,6-diamidino-2-phenylindole; blue). Scale bars, 20 μm. (**e**) F1 plants have a greatly reduced number of seeds per silique over the whole length of inflorescence (silique position is counted from proximal to distal end of inflorescence), as compared with wild-type and parental lines. Five plants were analysed for each line and the mean numbers of seeds per silique were plotted. Error bars indicate s.e.m. (shown for F1 only; did not exceed 10% of the mean for all other measurements). (**f**, **g**) Ovule abortion in F1 plants. (**f**) Both seeds and ovules were observed in siliques collected 24 h after fertilization. Scale bars, 1 mm. (**g**) Only 25% of ovules developed to seeds in F1 plants. (**h**, **i**) Embryo lethality in F1 plants. (**h**) Developing siliques in F1 plants contained defective seeds of white or pale-yellow colour (arrow). Scale bars, 1 mm. (**i**) Pairs of differential interference contrast images of embryos in normal and defective seeds isolated from the same silique. Degradation of embryos in defective seeds occurred early in development, before the heart stage. Scale bars, 15 μm. WT, wild type.

containing almost no dying cells (Fig. 2d). Proteolysis of endogenous PaTSN correlated with metacaspase activity, reaching the maximum level in early embryos and declining to non-detectable levels in mature embryos (Fig. 2d). Furthermore, the molecular pattern of PaTSN fragmentation *in vivo* was similar to the *in vitro* cleavage of PaTSN by mcII-Pa (Fig. 2a, d). We microsurgically separated the embryonal masses from the suspensors and found that metacaspase activity was tenfold higher in the dying suspensors than the living embryonal masses (Fig. 2e). Accordingly, endogenous PaTSN was cleaved in the suspensors, but was intact in the embryonal masses. Knockdown of *mcII-Pa* by RNA interference (RNAi;

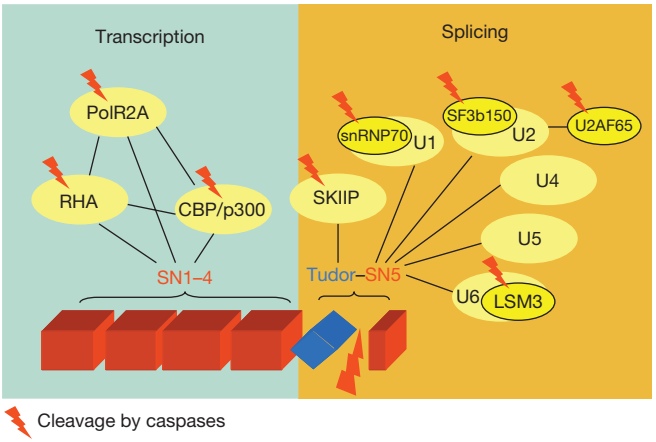

Figure 5 A proposed mechanistic model of caspase-mediated cleavage of TSN during PCD. Mammalian TSN couples transcription and splicing via interactions, through distinct domains, with key components of both processes. N-terminal SN1–4 domains interact with several components of the basal transcription machinery, including ATP-dependent RNA helicase A (RHA)[33], DNA-directed RNA polymerase II largest subunit (PolR2A) and CREB-binding protein (CBP/p300). C-terminal Tudor and SN5 domains interact with core components involved in RNA splicing, including protein components of U1, U2, U4, U5 and U6 small nuclear ribonucleoproteins (snRNPs)[15] and nuclear protein SKIP (SKIIP). Caspase-mediated cleavage of TSN between the Tudor and SN5 domains impairs TSN interaction with spliceosome components and, consequently, splicing, uncoupling transcription from splicing. These changes may lead to the perturbation of the expression of genes involved in maintaining the balance between cell survival and death. Several components of transcription and splicing machineries are known substrates of caspases. Interactions between proteins and protein complexes are denoted by black lines. Four spliceosome core proteins that are targeted by caspases, U1 snRNP relative molecular mass M_r 70K (snRNP70), splicing factor 3B subunit 2 (SF3b150), splicing factor U2AF 65K subunit (U2AF65) and U6 snRNA-associated Sm-like protein LSm3 (LSM3), do not interact directly with TSN but belong to TSN-interacting protein complexes (see Methods for annotation databases).

Supplementary Information, Fig. S3d) resulted in partial or complete inhibition of PaTSN cleavage, depending on the level of remaining metacaspase activity (Fig. 2f). These data demonstrate that PaTSN is a substrate for metacaspase mcII-Pa and is a component of the degradome during developmental PCD.

To test whether PaTSN is also a part of the stress-induced cell-death degradome, embryogenic cells of *P. abies* were treated with hydrogen peroxide in the presence of growth factors that promote cell proliferation while suppressing embryonic patterning and developmental PCD[27]. Metacaspase activity increased for up to 12 h of incubation with hydrogen peroxide and then gradually decreased during further incubation, concomitant with the progression of cell death (Fig. 2g). The increase in metacaspase activity was accompanied by enhanced cleavage of endogenous PaTSN, in a pattern similar to that in *in vitro* assays and developmental PCD (Fig. 2a, d–g). Therefore, we conclude that PaTSN is a part of the degradome during both developmental and stress-induced cell deaths.

Participation of HsTSN in the activation of transcription and splicing relies on its interaction with large molecular complexes, which requires TSN to be intact[10,13,15]. In particular, HsTSN accelerates the kinetics of spliceosome assembly through interaction with small nuclear ribonucleoproteins (snRNPs) that function in pre-mRNA splicing[15]. This interaction is mediated by the carboxy-terminal TSN region, which consists of a hook-like structure formed by the Tudor and SN5 domains[28]. An aromatic cage within the hook binds methyl groups of snRNPs, anchoring TSN to the spliceosome. As caspase-mediated cleavage after Asp 790 (within the α2 helix and between the Tudor and SN5 domains) disrupts the hook structure (Fig. 3a), it may impair the function of TSN. We compared the effect of full-length TSN versus its N- and C-terminal cleavage products on the kinetics of *in vitro* spliceosome assembly, using a radiolabelled splicing substrate (pre-mRNA). As found previously[15], full-length TSN accelerated spliceosome assembly and pre-mRNA splicing *in vitro* (Fig. 3b, lanes 5–8). In the control reactions (Fig. 3b, lanes 1–4), the pre-spliceosomal complex A was detected at 5 min and peaked at 30 min, whereas the fully assembled spliceosomal complex B was clearly detected after 30 min (Fig. 3b, c). In the presence of intact TSN, complex A detection had already peaked by 10 min and the kinetic appearance of complex B (detected by 5 min) was similarly accelerated (Fig. 3b, c). This was especially apparent at the early time points when there was up to a threefold difference between B complex formation in the presence and absence of intact TSN (Fig. 3d). The N-terminal TSN fragment (Fig. 3b, lanes 9–12) had a mild stimulatory effect on complex A, but not complex B, formation (Fig. 3c, d). The kinetics of reactions containing the C-terminal TSN fragment alone (Fig. 3b, lanes 13–16) or together in equimolar amounts with the N-terminal fragment (Fig. 3b, lanes 17–20) were similar to that of the control reaction (Fig. 3c, d). Therefore, caspase-mediated cleavage of TSN between the Tudor and SN5 domains inhibits its stimulatory function in pre-mRNA splicing. Molecular modelling predicts that the cleavage also generates a surface-exposed hydrophobic area (Fig. 3a), which might induce protein aggregation leading to inhibition of other TSN functions.

Besides being a transcription and splicing activator, animal TSN is a nuclease that resides in both the RISC[11] and stress granules[14] and, in the latter case, is directly responsible for the degradation of edited double-stranded RNA. To investigate whether TSN cleavage compromises its nucleolytic function, we assessed ribonuclease activity of intact versus cleaved TSN. Nuclease activity of both HsTSN and PaTSN was highly sensitive to pdTp (3′, 5′-deoxythymidine bisphosphate), a specific inhibitor of SN[11,12], whereas the inactive analogue dTp (3′-deoxythymidine monophosphate) had no inhibitory effect (Fig. 3e, f). Cleavage of HsTSN by caspase-3 lowered its nuclease activity by almost 50% and, consistent with this, DEVD-CHO-inactivated caspase-3 did not affect HsTSN activity (Fig. 3e). Cleavage of PaTSN by mcII-Pa led to a 90% decrease in ribonuclease activity, whereas inactivation of mcII-Pa by either EGR-cmk or mutation of catalytic Cys 139 left TSN intact and fully active (Fig. 3f). As pdTp inhibits the nuclease activity of TSN, it can be used to mimic the effect of TSN cleavage *in vivo*. Treatment of early *P. abies* embryos with pdTp caused a fourfold increase in the frequency of embryonal masses containing fragmented nuclear DNA, as revealed by a TUNEL assay (Supplementary Information, Fig. S3e, f). The nuclease activity of TSN is therefore essential for cell viability.

The conservation between plant and animal TSN sequences, and their comparable SN-like activity suggest that plant TSN might perform similar functions to its animal counterpart. However, immunolocalization in early *P. abies* embryos revealed that PaTSN does not localize to the nucleus, but resides in the cytoplasm during both interphase and mitosis (Supplementary Information, Fig. S4a, b), indicating that plant TSN is unlikely to be involved in transcriptional regulation and splicing.

Reverse genetics were used to study plant TSN further. The *Arabidopsis* genome has two TSN homologues, *AtTSN1* (At5g61780) and *AtTSN2*

(At5g07350), and both contain all four metacaspase cleavage sites identified in PaTSN (Supplementary Information, Fig. S2c). Moreover, similarly to PaTSN, *Arabidopsis* TSN localizes to the cytoplasm in interphase and mitosis (Supplementary Information, Fig. S4c). We isolated two transfer DNA (T-DNA) knockout alleles for each *TSN* gene (Supplementary Information, Fig. S5) and found no discernible developmental defects in the homozygous lines, except for an 8–16% reduction in fertility. Double heterozygous plants from all four crosses revealed no vegetative defects, but their flowers had short stamens and low quantities of pollen (Fig. 4a). The amount of viable pollen grains was reduced by 85–89% from that of wild-type and parental plants (10 stamens from 3 plants of each line were analysed). Although the early stages of pollen development appeared to proceed normally, starting from flower stage 11, most pollen grains showed typical cytological hallmarks of plant PCD[26,29], including formation of large vacuoles and nuclear condensation (Fig. 4b, c). In addition, nuclear DNA was fragmented in 32% of pollen grains (Fig. 4d), providing compelling evidence for PCD-mediated pollen degeneration. A high frequency of non-viable pollen detected in F1 plants is inconsistent with a male gametophyte-lethal mutation (25% of pollen abortion if double heterozygote), demonstrating a sporophytic requirement[30]. Consistent with this, *in situ* hybridization analysis revealed accumulation of *AtTSN1* and *AtTSN2* transcripts in tapetal cells (Supplementary Information, Fig. S4d–j), which surround male gametophytes and are essential for pollen production[31].

The fertility of F1 plants was impaired, resulting in a 70–98% reduction in the number of seeds (Fig. 4e). Examination of siliques 24 h after fertilization showed that development of 75% of ovules on F1 plants was arrested (Fig. 4f, g). Furthermore, 8% of seeds on F1 plants were aborted during subsequent developmental stages (Fig. 4h) and embryogenesis in these seeds was arrested before the heart stage (Fig. 4i). Out of 100 genotyped F2 plants, none were homozygous for both T-DNA alleles, suggesting that knockout of both *TSN* genes is lethal. Downregulation of *AtTSN* using RNAi resulted in pollen degeneration and a dramatic reduction in plant fertility (Supplementary Information, Fig. S6), providing further evidence for an essential role of TSN in plant reproduction.

PCD plays a fundamental part in plant biology, but the exact molecular pathways responsible for cell dismantling remain poorly understood. Two groups of cysteine proteases have recently been shown to represent key executioners of PCD in plants. The first group includes vacuolar processing enzymes, which may be responsible for the growth and rupture of lytic vacuoles[32]. The second group encompasses the metacaspases, which localize both to the nucleus and cytoplasm, and execute nuclear and cytoplasmic degradation before vacuolar collapse[6]. Identification of the natural substrates for these proteases is essential to understanding the PCD mechanisms in plants and the evolution of the PCD machinery. Here we report TSN as the first natural substrate cleaved *in vivo* by a metacaspase. We demonstrate that TSN has ribonuclease activity essential for plant viability, as downregulation of this activity, either by a specific inhibitor or by reverse genetics, results in ectopic cell death in flowers and embryos. This activity of TSN can also be impaired by metacaspase-mediated cleavage during PCD.

Whereas plant TSN is a substrate of metacaspases and is essential for cell viability and reproduction, its mammalian homologue is targeted by caspases during apoptosis and has an important role as proliferative and pro-survival factor. However, it remains unknown how TSN cleavage compromises cell viability. It has been shown that the N-terminal SN1–4 domains of mammalian TSN interact with several components of the basal transcription machinery, whereas the C-terminal hook-like region, composed of Tudor and SN5 domains, interacts with splicing factors and facilitates spliceosome assembly (Fig. 5). Thus, TSN bridges transcription and splicing[15,28]; therefore cleavage by effector caspases will not only disrupt the hook region, preventing the stimulation of spliceosome assembly, but will also uncouple these two processes. Interestingly, most of the TSN partner proteins in transcription and splicing are themselves cleaved by caspases (Fig. 5), demonstrating that caspases target several components of protein complexes to ensure efficient dysregulation of vital cellular functions. Unlike animal cell death systems, cleavage of plant TSN by metacaspases breaks it into several fragments and will probably inactivate its nucleolytic activity as well as all other TSN functions. Therefore, despite distinct enzymatic properties and phylogenetic distance, caspases and metacaspases can target common molecules in the cell, highlighting evolutionary conservation of PCD degradomes in plants and animals. □

METHODS

Methods and any associated references are available in the online version of the paper at http://www.nature.com/naturecellbiology/.

Note: Supplementary Information is available on the Nature Cell Biology website.

ACKNOWLEDGEMENTS

The authors thank: L. Filonova (Swedish University of Agricultural Sciences) for microsurgery preparations of plant embryos; G. Swärdh (Swedish University of Agricultural Sciences) for *Arabidopsis* transformation and J. Dangl, A. Jones, C. Knorpp and S. Orrenius for comments on the manuscript. This work was supported by the Swedish Research Council (VR), the Swedish Cancer Society, the Swedish Research Council for Environment, Agricultural Sciences and Spatial Planning (Formas), the EC FP6 and FP7 Programs, the Carl Tryggers Foundation, the Pehrssons Fund, the Wenner-Gren Foundation, the Royal Swedish Academy of Agriculture and Forestry and the Ministerio de Ciencia e Innovacion, Spain. A.V. is a postdoctoral fellow of the Wenner-Gren Foundation.

AUTHOR CONTRIBUTIONS

A.P.S, E.S., B.Z. and P.V.B. designed the research; J.F.S., A.V., A.P.S., E.I.S., A.G., E.M., B.S.T., S.R-N., A.A.Z.Jr, T.V., J.S., M.J.F., M.F.S., A.Z., U.S., E.S. and P.V.B. performed experiments and analysed data; P.J.H. and O.S. contributed new reagents/analytic tools; A.P.S., E.S., B.Z. and P.V.B. coordinated the study; A.P.S., O.S., B.Z. and P.V.B. wrote the paper; P.V.B. was responsible for the overall project.

COMPETING FINANCIAL INTERESTS

The authors declare no competing financial interests.

Published online at http://www.nature.com/naturecellbiology/.
Reprints and permissions information is available online at http://npg.nature.com/reprintsandpermissions/.

1. Lopez-Otin, S. & Overall, C. M. Protease degradomics: a new challenge for proteomics. *Nature Rev. Mol. Cell Biol.* **3,** 509–519 (2002).
2. Fischer, U., Jänicke R. U. & Schulze-Osthoff, K. Many cuts to ruin: a comprehensive update of caspase substrates. *Cell Death Differ.* **10,** 76–100 (2003).
3. Uren, A. G. *et al.* Identification of paracaspases and metacaspases: two ancient families of caspase-like proteins, one of which plays a key role in MALT lymphoma. *Mol. Cell* **6,** 961–967 (2000).
4. Vercammen, D., Declercq, W., Vandenabeele, P. & Van Breusegem, F. Are metacaspases caspases? *J. Cell Biol.* **179,** 375–380 (2007).
5. Suarez, M. F. *et al.* Metacaspase-dependent programmed cell death is essential for plant embryogenesis. *Curr. Biol.* **14,** R339–R340 (2004).
6. Bozhkov, P. V. *et al.* Cysteine protease mcII-Pa executes programmed cell death during plant embryogenesis. *Proc. Natl Acad. Sci. USA* **102,** 14463–14468 (2005).
7. He, R. *et al.* Metacaspase-8 modulates programmed cell death induced by UV and H202 in *Arabidopsis*. *J. Biol. Chem.* **283,** 774–783 (2008).
8. Van der Hoorn, R. A. L. Plant proteases: from phenotypes to molecular mechanisms. *Annu. Rev. Plant Biol.* **59,** 191–223 (2008).
9. Tong, X., Drapkin, R., Yalamanchill, R., Mosialos, G. & Kieff, E. The Epstein-Barr virus nuclear protein 2 acidic domain forms a complex with a novel cellular coactivator that can interact with TFIIE. *Mol. Cell Biol.* **15,** 4735–4744 (1995).

10. Yang, J. *et al.* Identification of p100 as a coactivator for STAT6 that bridges STAT6 with RNA polymerase II. *EMBO J.* **21,** 4950–4958 (2002).
11. Caudy, A. A. *et al.* A micrococcal nuclease homologue in RNAi effector complexes. *Nature* **425,** 411–414 (2003).
12. Scadden, A. D. J. The RISC subunit Tudor-SN binds to hyper-edited double-stranded RNA and promotes its cleavage. *Nature Struct. Mol. Biol.* **12,** 489–496 (2005).
13. Välineva, T., Yang, J., Palovuori, R. & Silvennoinen, O. The transcriptional co-activator protein p100 recruits histone acetyltransferase activity to STAT6 and mediates interaction between the CREB-binding protein and STAT6. *J. Biol. Chem.* **280,** 14989–14996 (2005).
14. Scadden, A. D. J. Inosine-containing dsRNA binds a stress-granule-like complex and downregulates gene expression in trans. *Mol. Cell* **28,** 491–500 (2007).
15. Yang, J. *et al.* Transcriptional co-activator protein p100 interacts with snRNP proteins and facilitates the assembly of the spliceosome. *Nucleic Acids Res.* **35,** 4485–4494 (2007).
16. Callebaut, I. & Mornon J. P. The human EBNA-2 coactivator p100: multidomain organization and relationship to the staphylococcal nuclease fold and to the tudor protein involved in *Drosophila melanogaster* development. *Biochem J.* **321,** 125–132 (1997).
17. Talanian, R. V. *et al.* Substrate specificities of caspase family proteases. *J. Biol. Chem.* **272,** 9677–9682 (1997).
18. Enari, M. *et al.* A caspase-activated DNase that degrades DNA during apoptosis, and its inhibitor ICAD. *Nature* **391,** 43–50 (1998).
19. Vercammen, D. *et al.* Type II metacaspases Atmc4 and Atmc9 of *Arabidopsis thaliana* cleave substrates after arginine and lysine. *J. Biol. Chem.* **279,** 45329–45336 (2004).
20. Watanabe, N. & Lam, E. Two *Arabidopsis* metacaspases AtMCP1band AtMCP2b are arginine/lysine-specific cysteine proteases and activate apoptosis-like cell death in yeast. *J. Biol. Chem.* **280,** 14691–14699 (2005).
21. Vercammen, D. *et al.* Serpin1 of *Arabidopsis thaliana* is a suicide inhibitor for metacaspase 9. *J. Mol. Biol.* **364,** 625–636 (2006).
22. Madeo, F. *et al.* A caspase-related protease regulates apoptosis in yeast. *Mol. Cell* **9,** 911–917 (2002).
23. Kosec, G. *et al.* Metacaspases of *Trypanosoma cruzi*: possible candidates for programmed cell death mediators. *Mol. Biochem. Parasitol.* **145,** 18–28 (2006).
24. Earnshaw, W. C., Martins, L. M. & Kaufmann, S. H. Mammalian caspases: structure, activation, substrates, and functions during apoptosis. *Annu. Rev. Biochem.* **68,** 383–424 (1999).
25. Smertenko A. P., Bozhkov, P. V., Filonova, L. H., von Arnold, S. & Hussey, P. J. Reorganization of the cytoskeleton during developmental programmed cell death in *Picea abies* embryos. *Plant J.* **33,** 813–824 (2003).
26. Bozhkov, P. V., Filonova, L. H. & Suarez, M. F. Programmed cell death in plant embryogenesis. *Curr. Top. Dev. Biol.* **67,** 135–179 (2005).
27. Filonova, L. H. *et al.* Two ways of programmed cell death occur during formation and development of somatic embryos in the gymnosperm, Norway spruce. *J. Cell Sci.* **113,** 4399–4411 (2000).
28. Shaw, N. *et al.* The multifunctional human p100 protein 'hooks' methylated ligands. *Nature Struct. Mol. Biol.* **14,** 779–784 (2007).
29. Hofius, D., Tsitsigiannis, D. I., Jones, J. D. & Mundy, J. Inducible cell death in plant immunity. *Semin. Cancer Biol.* **17,** 166–187 (2007).
30. Howden, R. *et al.* Selection of T-DNA-tagged male and female gametophytic mutants by segregation distortion in *Arabidopsis. Genetics* **149,** 621–631 (1998).
31. Koltunow, A. M., Truettner, J., Cox, K. H., Wallroth, M. & Goldberg, R. B. Different temporal spatial gene expression patterns occur during anther development. *Plant Cell* **2,** 1201–1224 (1990).
32. Hara-Nishimura, I., Hatsugai, N., Nakaune, S., Kuroyanagi, M. & Nishimura, M. Vacuolar processing enzyme: an executor of plant cell death. *Curr. Opin. Plant Biol.* **8,** 404–408 (2005).
33. Välineva, T., Yang, J. & Silvennoinen, O. Characterization of RNA helicase A as component of STAT6-dependent enhanceosome. *Nucleic Acids Res.* **34,** 3938–3946 (2006).

METHODS

Gene cloning and phylogenetic analysis. To clone full-length cDNA for Pa*TSN*, 5′- and 3′-RACE-PCR combined with nested PCR was performed using total RNA extracted from early embryos. Degenerated nested oligonucleotides (5′-CCTGGTGCTNCWGARGMATC-3′ and 5′-CATRYTNGCACTCCAHTCAAC-3′) were designed from the conserved region in the second SN-domain found in plant TSN sequences. Cloning of HsTSN cDNA was performed as described previously[9]. For the D790E mutation, QuickChange site-directed mutagenesis kit (Stratagene) was used. The phylodendrogram of TSN proteins was constructed with PAUP software using neighbour joining and maximal parsimony algorithms. Both algorithms produced similar phylodendrograms.

Recombinant proteins. Wild-type and C139A mutant mcII-Pa were expressed in *Escherichia coli* and purified as described previously[6]. Active recombinant human caspase-3 was from BD Pharmingen. Full-length HsTSN, Pa*TSN* and At*TSN1* cDNAs were cloned into a EcoRI/HindIII-digested pET28a vector (Novogen). The recombinant proteins were expressed as described previously[6], except that HEPES was used instead of Tris and phosphate. The purified proteins were dialysed overnight against HEPES (50 mM at pH 7.8), NaCl (50 mM), dithiothreitol (DTT; 1 mM) and 10% (v/v) glycerol and then additionally purified by anion exchange chromatography on a Q Sepharose Fast Flow column (Pharmacia) using a linear gradient of NaCl (0–500 mM) in Tris-HCl (20 mM at pH 8.0), DTT (2 mM) and 10% (v/v) glycerol.

***In vitro* TSN cleavage assays and fragment sequencing.** Caspase-3 and mcII-Pa induced cleavage of HsTSN and PaTSN, respectively, were assayed in 10-µl reactions containing recombinant TSN (30 pmol), protease (1.5 pmol, caspase-3 or mcII-Pa), HEPES (100 mM at pH 7.0), DTT (5 mM) and 0.1% (v/v) 3-[(3-cholamidopropyl) dimethylammonio]-1-propanesulfonate (CHAPS). For mcII-Pa catalysis, the reactions were supplemented with $CaCl_2$ (50 mM)[6]. For inhibition assays, 20 µM of either DEVD-CHO (Peptide Institute) or EGR-cmk (Bachem) were added. The proteins were incubated for 2 h at 28 °C, separated by 4-15% gradient SDS–PAGE and stained by Coomassie blue.

For terminal sequencing of TSN fragments, the reactions were scaled up proportionally to achieve 0.6 and 6 nmol TSN for N-terminal and C-terminal sequencing, respectively. The cleaved TSN proteins were subjected to 4-15% gradient SDS–PAGE, blotted onto polyvinilidene difluoride (PVDF) membrane (Applied Biosystems), and stained according to the manufacturer's instructions for sequencing.

Human cell lines. HCT116 human colon carcinoma cells and human embryonal kidney cells HEK293 (both from ATCC) were grown in Dulbecco's modified Eagle's medium (DMEM; Gibco) supplemented with 10% (v/v) heat-inactivated foetal calf serum, glutamine (4 mM), penicillin (100 U ml^{-1}) and streptomycin (100 µg ml^{-1}; all from Gibco). Human cervix adenocarcinoma HeLa cells (ATCC) were cultured in MEM medium with Earle's salts supplemented with NEAA (0.1 mM), pyruvate (1 mM), glutamine (4 mM), penicillin (100 U ml^{-1}), streptomycin (100 µg ml^{-1}), and 10% (v/v) foetal calf serum. All cell lines were maintained at 37 °C in a 5% CO_2, 95% air-humidified incubator.

For expression experiments, *HsTSN* gene was amplified with the pair of primers: (i) 5′-GGATCCATGGTCCTCTCAGGGTGC-3' and (ii) 5'-GAATTCTTAGCGGCTGTAGCCAAATTC-3' and cloned into *Bam*HI-*Eco*RI sites of pCMV-Tag2 plasmid (Stratagene). $HsTSN^{D790E}$ mutant was produced using QuickChangeTM site-directed mutagenesis kit (Stratagene). For transfection, 10^5 cells per well were seeded in 12-well plates in growth medium without antibiotics. Twenty-four hours after seeding, cells were transfected with a DNA:Lipofectamine 2000 (Invitrogen) mixture at a 2 µg:2 µl ratio. To estimate transfection efficiency, cells were co-transfected with a pEGFP-N1 vector and cells with EGFP fluorescence were counted 24 h and 48 h after transfection using flow cytometry and fluorescence microscopy. In all experiments transfection efficiency was above 80%.

siRNA experiments. HeLa cells were seeded into 12-well plates at a final density of 70,000 cells per well in 800 µl of growth medium without antibiotics. To inhibit TSN expression, *TSN*-specific siRNA (sense: 5′-UCC ACU CGU UGC CUU UGC AUC UCC A-3′; antisense: 5′-UGG AGA UGC AAA GGC AAC GAG UGG A-3′) was designed as recommended by Invitrogen. ON-TARGET*plus* Non-targeting Pool (Cat. No. D-001810-10; Dharmacon) and Negative stealth siRNA control (Cat. No. 12935112; Invitrogen) were used as negative controls. All siRNAs were diluted in Opti-MEM I medium (100 µl; Gibco) and Lipofectamine 2000 reagent (1 µl; Invitrogen) was mixed with OptiMEM I medium (100 µl). Diluted siRNA and Lipofectamine 2000 were mixed, incubated for 20 min, and added to each well 24 h after seeding. The final concentration of siRNA was 50 nM. After 24 h, the medium was exchanged for a fresh one supplemented with 10% (v/v) foetal calf serum, without antibiotics. Forty-eight hours after transfection, the cells were treated with CPT (final concentration 7.5 µM) or DMSO (vehicle) for 5 h and collected for further analyses.

Plant embryogenesis system. The *P. abies* wild-type embryogenic cell line 95.88.22 and *mcII-Pa*-silenced clones[5] were cultured as described previously[27]. The embryonal masses were separated from the suspensors in 7-day-old embryos using surgical blades in droplets of culture medium viewed under a binocular microscope.

T-DNA insertion lines and RNAi. *Arabidopsis* T-DNA insertion lines *tsn1-1, tsn1-2* and *tsn2-1* were obtained from SALK collection, stock numbers SALK143497, SALK052200 and SALK045179, respectively. T-DNA insertion line *tsn2-2* was from Cold Spring Harbor Laboratories collection, stock number CSHLET12646. Binary hairpin RNA pAGRIKOLA vector was purchased from the Nottingham Arabidopsis Stock Center (NASC). The construct was validated and sequenced with four AGRIKOLA primers (Agri51, Agri56, Agri64 and Agri69), and appeared to encompass a 231 nucleotide fragment (nucleotides 1735–1966) of *AtTSN1* (At5g61780), sharing 80.5% identity with the corresponding *AtTSN2* (At5g07350) gene fragment.

A *P. abies mcII-Pa* RNAi construct was prepared using 689-nucleotide-long sense and antisense arms corresponding to a 391-bp fragment of the p20-like caspasoide domain and a 298-bp fragment of the insert region showing the lowest similarity (from 31 to 64%) between plant metacaspase family proteases[5]. A BLAST search of spruce (*P. abies*) and pine (*Pinus taeda*) EST databases using this hairpin sequence as a bait revealed no hits, except for *mcII-Pa*.

Antibodies, immunoblotting, immunofluorescence and TUNEL. Anti-AtTSN1 was produced as described previously[6]. Mouse monoclonal anti-HsTSN was produced by FIT Biotech.

For immunoblotting, human cell monolayers were lysed in Complete lysis-M reagent (Roche) supplemented with protease inhibitor cocktail (Roche). Total plant proteins were extracted in Tris-HCl (250 mM at pH 6.8), 4% SDS, 20% glycerol and β-mercaptoethanol (1.5 M). Protein extracts were resolved by 4–15% gradient or 12% SDS–PAGE, transferred onto PVDF membrane (Amersham Pharmacia Biosciences) and probed with an anti-TSN (1:2,000 dilution), anti-Flag (1:2,000; Cat. No. F-1804, Sigma Aldrich), anti-cleaved caspase-3 (1:2,000; Cat. No. 9661, Cell Signaling Technology), anti-cleaved PARP (1:2,000; Cat. No. 9546, Cell Signaling Technology) or anti-cleaved lamin A (1:1,000; Cat. No. 2036, Cell Signaling Technology) antibody. Horseradish peroxidase-labelled anti-mouse-IgG or anti-rabbit-IgG (Pierce), both at a 1:10,000 dilution, were used as secondary antibodies. The signal was detected by enhanced chemiluminescence kit (Amersham Pharmacia Biosciences). An equal loading was verified using anti-glyceraldehyde-3-phosphate dehydrogenase (G3PDH) antibody (1:10,000; Cat. No. 2275, Biosite) for human protein extracts or with anti-actin (1:1,000; ICN) for plant protein extracts.

Immunofluorescence analysis combined with TUNEL and DAPI staining was performed on *P. abies* early embryos following the procedures described for mcII-Pa[6]. For TUNEL in flowers, samples were fixed in 4% paraformaldehyde (Sigma) and embedded in 100% Histowax (Histolab). Sections of 8 µm were cut using a HM 355S Microtome (MICROM International GmbH) and affixed to Probe-on Plus slides at 42° (Fisher Scientific). Histowax was removed by washing in xylene and sections were re-hydrated by washing in ethanol series (100% to 10%). After equilibration in PBS for 30 min, TUNEL was performed as described previously[6].

Protease activity assays. Cleavage of caspase substrate DEVD-AMC was measured as described previously[34]. *P. abies* cell extracts were prepared and assayed for mcII-Pa activity as previously described[6] using FESR-AMC substrate (50 µM; Anaspec), which was designed for the mcII-Pa zymogen autoprocessing site[6].

DOI: 10.1038/ncb1979

***In vitro* spliceosome analysis.** The analysis was conducted as described previously[15]. A plasmid encoding adenovirus major late transcription unit (AdML) pre-mRNA was provided by R. Reed (Harvard University, MA, USA). Plasmids used for bacterial production of the proteins for the spliceosome analysis were constructed by cloning PCR products corresponding to amino acids 1–910 (full-length mouse TSN), 1–815 (N-terminal fragment) and 816–910 (C-terminal fragment) into *Bam*HI and *Not*I sites of pGEX-4T-1 vector.

Nuclease activity assays. For electrophoretic assays, unlabelled single-stranded RNA substrates were generated by *in vitro* transcription as described previously[35]. The assays were performed in two steps. In the first step, recombinant TSN protein (2.5 pmol) was co-incubated with a protease (125 fmol) in the presence or absence of either DEVD-CHO (20 μM; caspase-3 inhibitor) or EGR-cmk (20 μM; mcII-Pa inhibitor) in 5 μl reactions containing HEPES (50 mM at pH 7.0), NaCl (100 mM), DTT (5 mM) and 0.1% CHAPS. Reactions containing HsTSN and caspase-3 were supplemented with $CaCl_2$ (5 mM), whereas reactions containing PaTSN and mcII-Pa were supplemented with $CaCl_2$ (30 mM). For TSN inhibition, pdTp (Jena Bioscience) or dTp (Sigma) were added to a final concentration 500 μM. The reactions were incubated for 2 h at 28°C. Under these conditions TSN was completely processed, as verified by SDS–PAGE. Then, the volume of all reactions was adjusted to 15 μl with buffer containing HEPES (50 mM at pH 7.0), NaCl (100 mM), $CaCl_2$ (5 mM), ATP (1.5 mM) and substrate RNA (75 fmol), and the reactions were incubated for an additional 1 h at 28 °C. The integrity of RNA was analysed by native agarose gel electrophoresis in the presence of ethidium bromide.

For quantification of TSN ribonuclease activity, the reactions were set up as described above, except that unlabelled RNA substrates were substituted by fluorescently-labelled single-stranded RNA substrate (1–2 pmol) from fluorometric RNase detection assay (Ambion). The fluorescence was measured on VersaFluor fluorometer (BioRad) using excitation/emission wavelengths 490/520 nm and was directly proportional to the ribonuclease activity. Reactions containing Ribonuclease A (Ambion) and fluorescent RNA substrate were used for calibration and conversion of fluorescence units to pmol RNA min^{-1} per mg protein.

Light and transmission electron microscopy. Fixation, embedding, sectioning and tissue preparation of *Arabidopsis* flowers and ovules was performed as described previously[36].

***In situ* hybridization.** mRNA *in situ* hybridization was performed as described previously[37]. Gene specific probes for *AtTSN1* were amplified using primers 5′-TCAGTGTTCCTTCCATCTCCTACC-3′ and 5′-CGTTCGTCTTTGAGTTTTTCTCCC-3′ whereas *AtTSN2* probes were amplified using primers 5′-CACCGTAGAAACCAGGCAAAAG-3′ and 5′-TCAACAGCAATGAGAGTGACAACG-3′. Template for transcription of *AtTSN1* and *AtTSN2* antisense probes was amplified using modified reverse primers carrying a T7-sequence promotor sequence. Template for transcription of *AtTSN1* and *AtTSN2* sense probes was amplified using forward primers carrying a T7-promotor sequence.

Northern blotting. Total RNA was isolated from *P. abies* wild-type and mcII-Pa RNAi cell lines using the CTAB method[38]. Ten micrograms of total RNA was separated on 1% agarose denaturing gels and transferred to Hybond-XL (GE Healthcare). Full-length cDNAs for mcII-Pa and actin were used as templates for synthesis of specific probes. [^{32}P]CTP-labelled probes were generated using NEBlot kit (N1500S, NEB). The membranes were probed overnight at 65 °C and washed under low stringency conditions: twice with 2×SSC and 0.1% SDS for 5 min at room temperature and then with 1×SSC and 0.1% SDS for 10 min at 65 °C. The signal was detected using Phosphoimager system (BioRad Laboratories).

Modelling. To model the HsTSN cleavage, the N-terminal amino and C-terminal carboxyl groups were recreated on Ser 791 and Asp 790, respectively. The local conformation of the protein was changed to relieve collisions between atoms. The distances were inspected and stereochemistry was fixed using the O program[39]. Graphics was generated using PyMol.

TSN-interacting proteins. These proteins are annotated in the Entrez (http://www.ncbi.nlm.nih.gov/sites/entrez) and Biogrid (http://www.thebiogrid.org/) databases, and caspase substrates are annotated in the CASBAH database (http://bioinf.gen.tcd.ie/casbah/).

Accession numbers. Gene bank accession numbers for the genes discussed in this paper are: *P. abies TSN*, AM398207; human *TSN*, U22055; *Arabidopsis TSN1*, At5g61780 and *TSN2*, At5g07350, and *P. abies mcII-Pa*, AJ534970. The Protein Data Bank accession number of human TSN is 204X.

34. Vakifahmetoglu, H., Olsson, M., Orrenius, S. & Zhivotovsky, B. Functional connection between p53 and caspase-2 is essential for apoptosis induced by DNA damage. *Oncogene* **25,** 5683–5692 (2006).
35. Kreuze, J. F., Savenkov, E. I., Cuellar, W., Li, X. & Valkonen, J. P. T. Viral class 1 RNase III involved in suppression of RNA silencing. *J. Virol.* **79,** 7227–7238 (2005).
36. Kuusk, S., Sohlberg J. J., Long, J. A., Fridborg, I. & Sundberg, E. STY1 and STY2 promote the formation of apical tissues during *Arabidopsis gynoecium* development. *Development* **129,** 4707–4717 (2002).
37. Karlgren, A., Carlsson, J., Gyllenstrand, N., Lagercrantz, U. & Sundström, JF. Non-radioactive *in situ* hybridization protocol applicable for Norway spruce and a range of plant species. *J. Vis. Exp.* **26,** 1205 (2009).
38. Chang, S., Puryear, J. & Cairney, J. A simple and efficient method for isolating RNA from pine trees. *Plant Mol. Biol. Reporter* **11,** 113–116 (1993).
39. Jones, T. A., Zou, J.-Y., Cowan, S. W. & Kjeldgaard, M. Improved methods for building protein models in electron desnity maps and the location of errors in these models. *Acta Cryst.* **A47,** 110–119 (1991).

nature cell biology

DOI: 10.1038/ncb1979

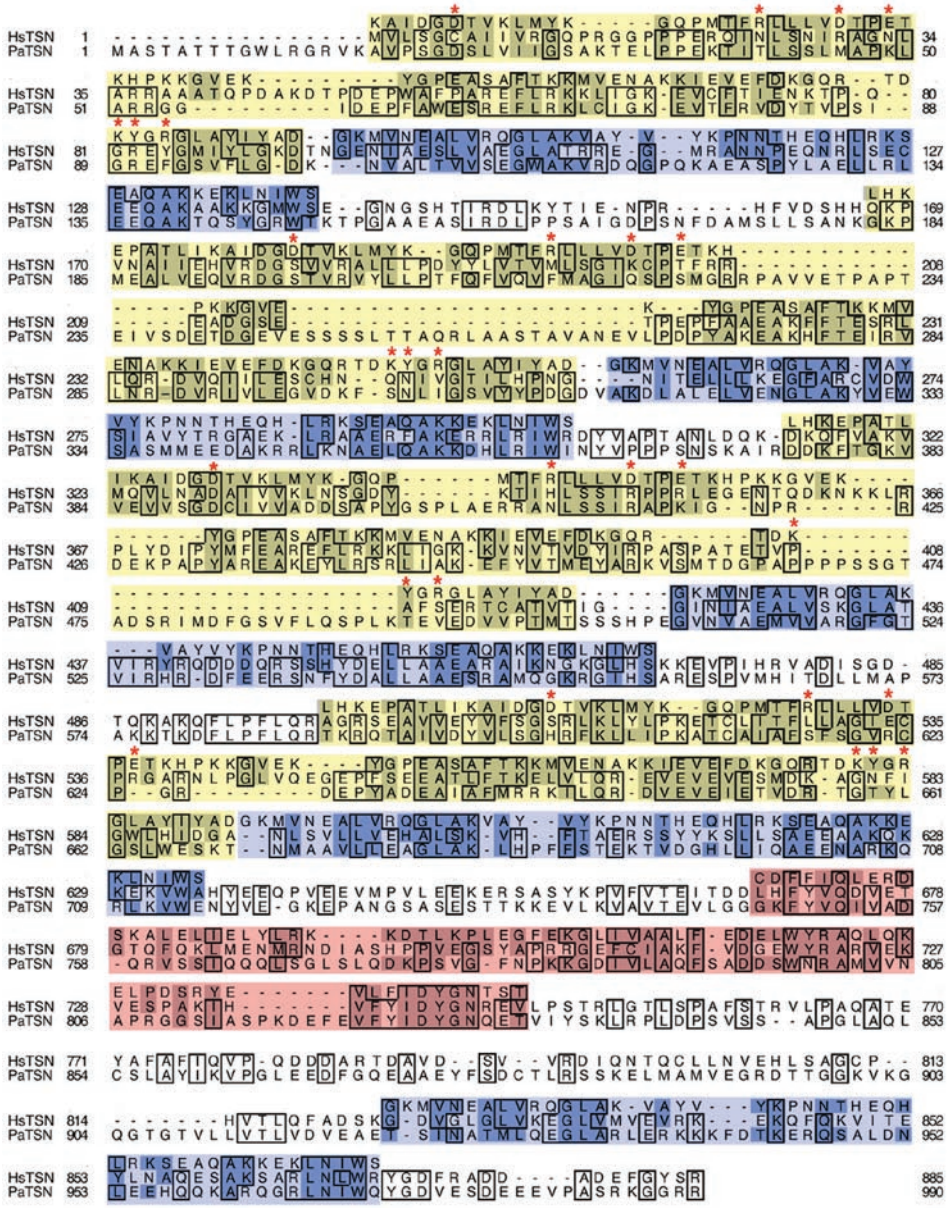

Figure S1 Alignment and domain composition of HsTSN and PaTSN. Since both HsTSN (accession number AAA80488) and PaTSN (accession number CAL38976) have five staphylococcal nuclease domains, each of them was aligned with the original *Staphylococcus aureus* nuclease sequence (accession number BAB56977) shown in the top row of the alignment. Full-length *S. aureus* nuclease has 228 amino acids, and one of each subdomains A and B. Regions homologues to *S. aureus* nuclease subdomain A or B are highlighted in yellow or blue, respectively. Highlighted in red is a region of TSN sequence homologous to Tudor V domain from the *Drosophila melanogaster* Tudor protein (accession number CAA44286), which is shown in the top row of the alignment. Identical and similar amino acid residues are boxed and grey shaded, respectively. Red asterisks denote amino acid residues important for nucleolytic activity of *S. aureus* nuclease.

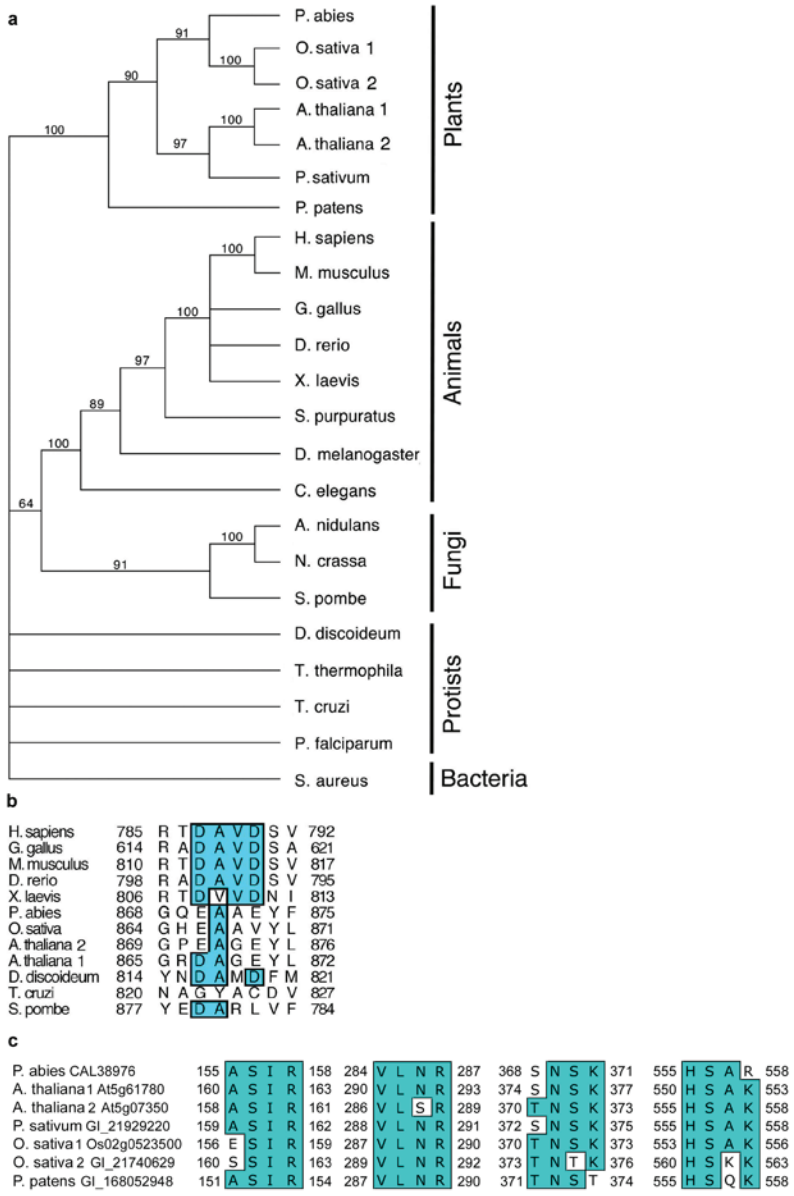

Figure S2 TSN proteins and their caspase-3 and metacaspase cleavage motives are evolutionarily conserved. (**a**) A bootstrap consensus of phylogenetic tree representing similarities of TSN protein sequences from *Picea abies* (accession number CAL38976), *Oryza sativa* 1 (accession number Os02g0523500) and 2 (accession number GI_21740629), *Physcomitrella patens* (accession number GI_168052948), *Pisum sativum* (accession number GI_21929220), *Arabidopsis thaliana* 1 (accession number At5g61780) and 2 (accession number At5g07350), *Homo sapiens* (accession number AAA80488), *Mus musculus* (accession number AAH07126), *Gallus gallus* (accession number AAL27548), *Danio rerio* (accession number AAH77133), *Xenopus laevis* (accession number AAH45115), *Strongylocentrotus purpuratus* (accession number XP_798852), *Drosophila melanogaster* (accession number NP_612021), *Caenorhabditis elegans* (accession number AAA81130), *Aspergillus nidulans* (accession number XP_657846), *Neurospora crassa* (accession number XP_964292), *Schizosaccharomyces pombe* (accession number CAB39904), *Dictyostelium discoideum* (accession number XP_641583), *Tetrahymena thermophila* (accession number EAR84819), *Trypanosoma cruzi* (accession number XP_964292), *Plasmodium falciparum* (accession number NP_701234) and nuclease from *Staphylococcus aureus* (accession number BAB56977). The tree was calculated with PAUP software using full heuristic search algorithm from the alignment of amino acid sequences generated by ClustalX software. The *S. aureus* nuclease was used as an outgroup sequence in order to root the phylogenetic tree. Altogether 1000 replicates of the trees were generated to calculate the bootstrap value and the minimum frequency value for the group retention was set up at 61%. A similar phylogenetic tree was obtained using Neighbour Joining algorithm. Note conservation of TSN sequence within major groups of organisms except protists. (**b**) The DAVD motif is only conserved in TSN proteins from vertebrates. Protein sequence alignment of regions containing caspase-3 cleavage motif (DAVD) in animals (*H. sapiens, M. musculus, G. gallus, D. rerio, X. laevis*) and corresponding region from plants (*P. abies, O. sativa, A. thaliana*), protists (*D. discoideum, T. cruzi*) and fungi (*S. pombe*). This is a fragment of alignment used to generate phylogenetic tree shown in **a**. The DAVD motif is only conserved in animals, but not in other species, although some plant and protists species have conserved amino acid substitutions in the corresponding positions. (**c**) All four metacaspase cleavage motives found in PaTSN are conserved in TSN from other higher plant species (note Arg or Lys are in the P1 position in all motives). In *P. patens* TSN, three out of four metacaspase cleavage motives are conserved.

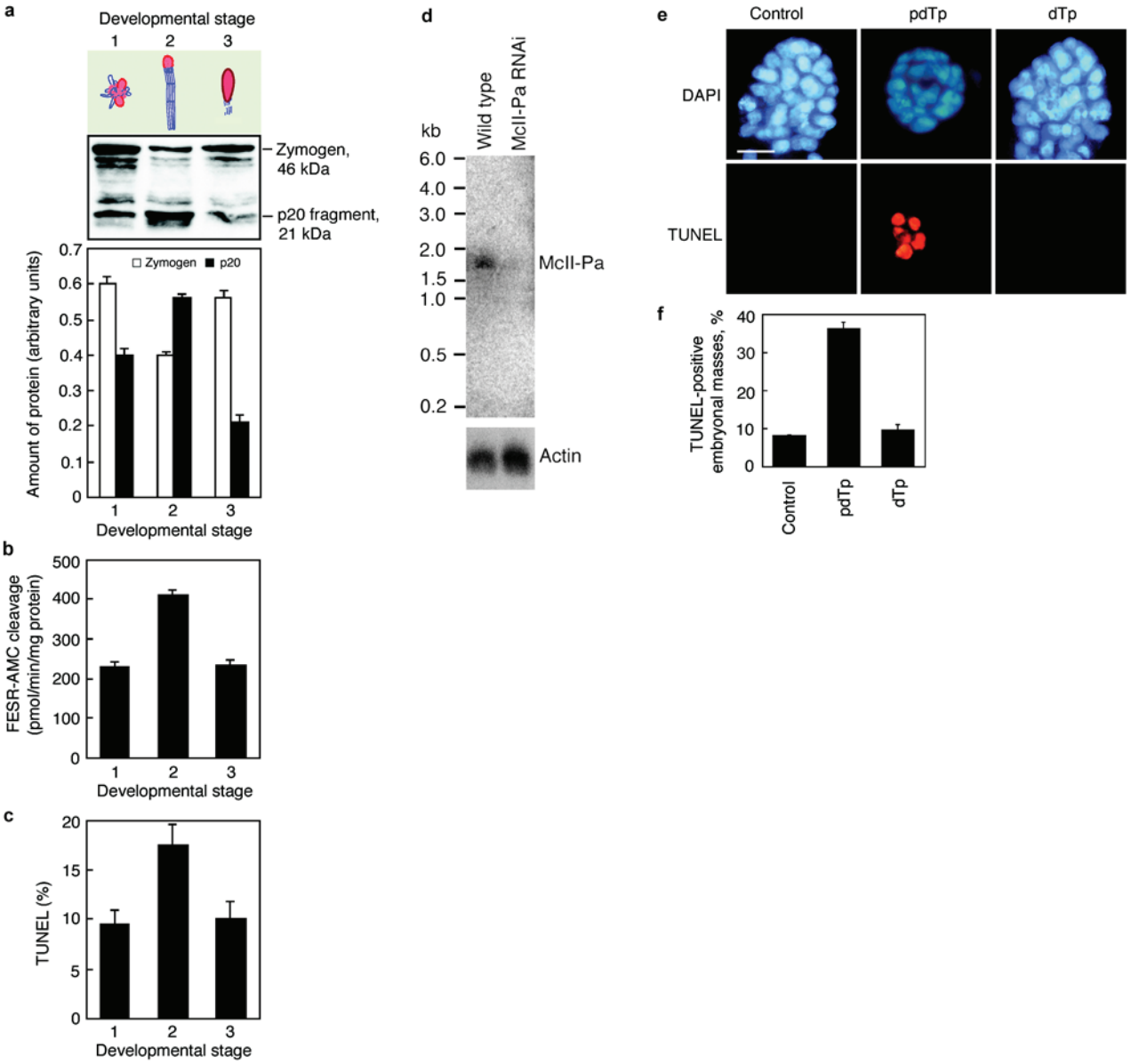

Figure S3 Analysis of mcII-Pa and TSN in *P. abies* embryos. (**a**) Total protein was extracted from embryogenic cells (stage 1), early embryos (stage 2) and late embryos (stage 3) and analysed by western blot using anti-mcII-Pa. The intensities of bands corresponding to zymogen and p20-like fragment were measured by densitometry. (**b**) Cleavage of FESR-AMC was measured fluorometrically in the cell extracts prepared from the same samples as in **a**. (**c**) The level of PCD was assessed as proportion of TUNEL-positive cells at the same developmental stages. In all three graphs the data show mean values of three independent measurements ± s.e.m. Processing of mcII-Pa zymogen yields catalytically active p20-like fragment. Accumulation of this fragment coincides with terminal differentiation and PCD of the embryo-suspensor at an early embryo stage (stage 2) and is accompanied by increase in proteolytic activity towards metacaspase peptidic substrate FESR-AMC. (**d**) Northern blot analysis of *mcII-Pa* in wild type and mcII-Pa RNAi cell lines. Note that type II metacaspase-specific probe detects a single band (ca. 1.7 kb) corresponding to the expected size of mcII-Pa transcript at low stringency of hybridization conditions. This band disappears in the RNAi line. Actin probe was used as a loading control. In addition, we have cloned and sequenced 150 cDNAs from embryonic mRNA and could not find any other metacaspase cDNAs than *mcII-Pa*. These results together with Northern blot data indicate that *mcII-Pa* is the only metacaspase gene expressed during *P. abies* embryogenesis. (**e, f**) Nucleolytic activity of TSN is essential for cell viability in the embryonal masses. The SN-specific inhibitor pdTp (500 μM) and its inactive analogue dTp (500 μM) were added to the embryogenic culture simultaneously with withdrawal of growth factors. Four days later, the embryos were analyzed for DNA fragmentation using double staining with DAPI and TUNEL. (**e**) Representative examples of the embryonal masses from each treatment. Scale bar, 50 μm. (**f**) The frequency of TUNEL-positive embryonal masses in each treatment. The embryonal mass was considered as TUNEL-positive if it contained at least two TUNEL-positive nuclei. Data represent the mean of three independent experiments ± s.e.m., and 500 embryos were scored at each replicate experiment.

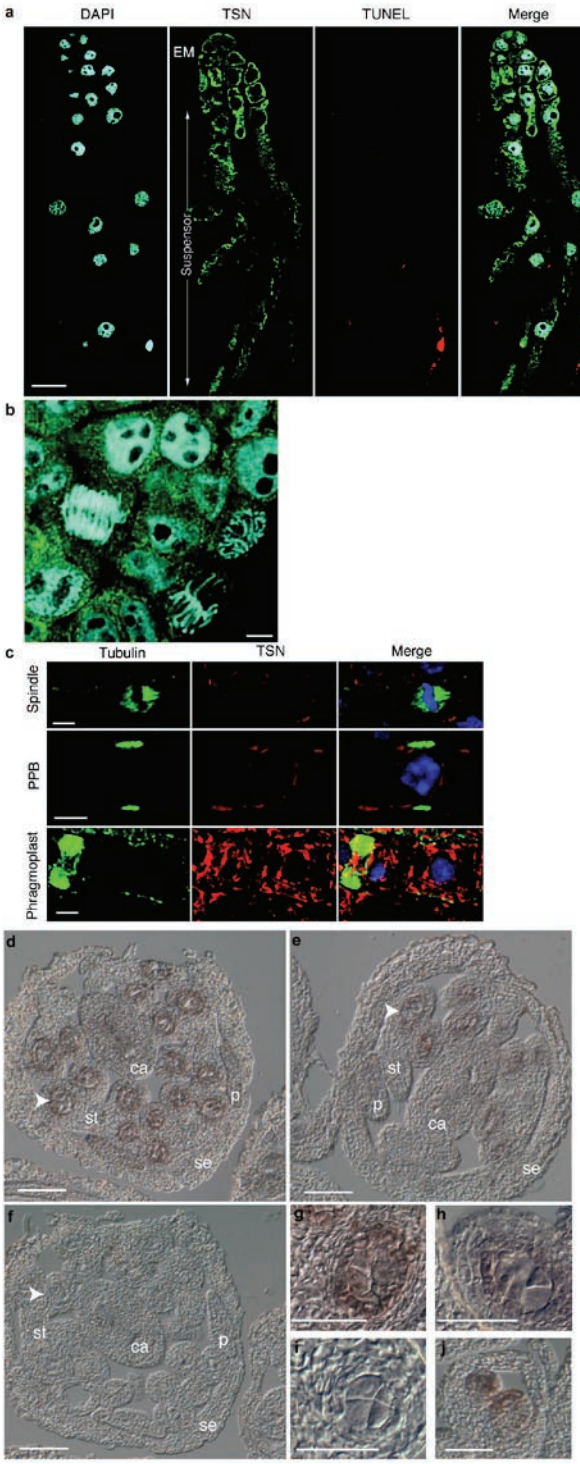

Figure S4 Localisation of TSN proteins and transcripts in plant cells and tissues**.** (**a-c**) Plant TSN is cytoplasmic in both living and dying cells. (**a**) Staining of nuclei with DAPI, immunolocalization of TSN, and detection of DNA fragmentation by TUNEL in *P. abies* embryos collected 7 days after withdrawal of growth factors. A representative example of one out of 50 embryos analyzed. EM, embryonal mass. Scale bar, 50 μm. (**b**) Immunolocalization of TSN (green staining) and nuclear staining with DAPI (blue) in the embryonal masses of *P. abies*. Note cytoplasmic signal of TSN in both interphase and mitotic cells. Scale bar, 10 μm. (**c**) Immunolocalization of TSN in *Arabidopsis* root tip cells counterstained with anti-α-tubulin to show the cell cycle stages. Note a lack of TSN co-localization with mitotic structures. PPB, preprophase band. Scale bars, 5 μm. (**d-j**) *AtTSN1* and *AtTSN2* transcripts accumulate in the tapetal cell layer of stage-9 wild type flowers. Micrographs show transverse sections of flowers hybridized with *AtTSN1* antisense probe (**d, g**), *AtTSN2* antisense probe (**e, h**), negative control *AtTSN1* sense probe (**f, i**) and positive control probe (**j**). Arrowheads in **d**, **e** and **f** point to tapetal cell layer that expresses *TSN* genes and are shown under higher magnification in **g**, **h** and **i**. Note a lack of the hybridization signal on the negative control section (**f, i**). ca, carpel; st, stamen; p, petal; se, sepal. Scale bars, 50 μm in **d-f** and 25 μm in **g-j**.

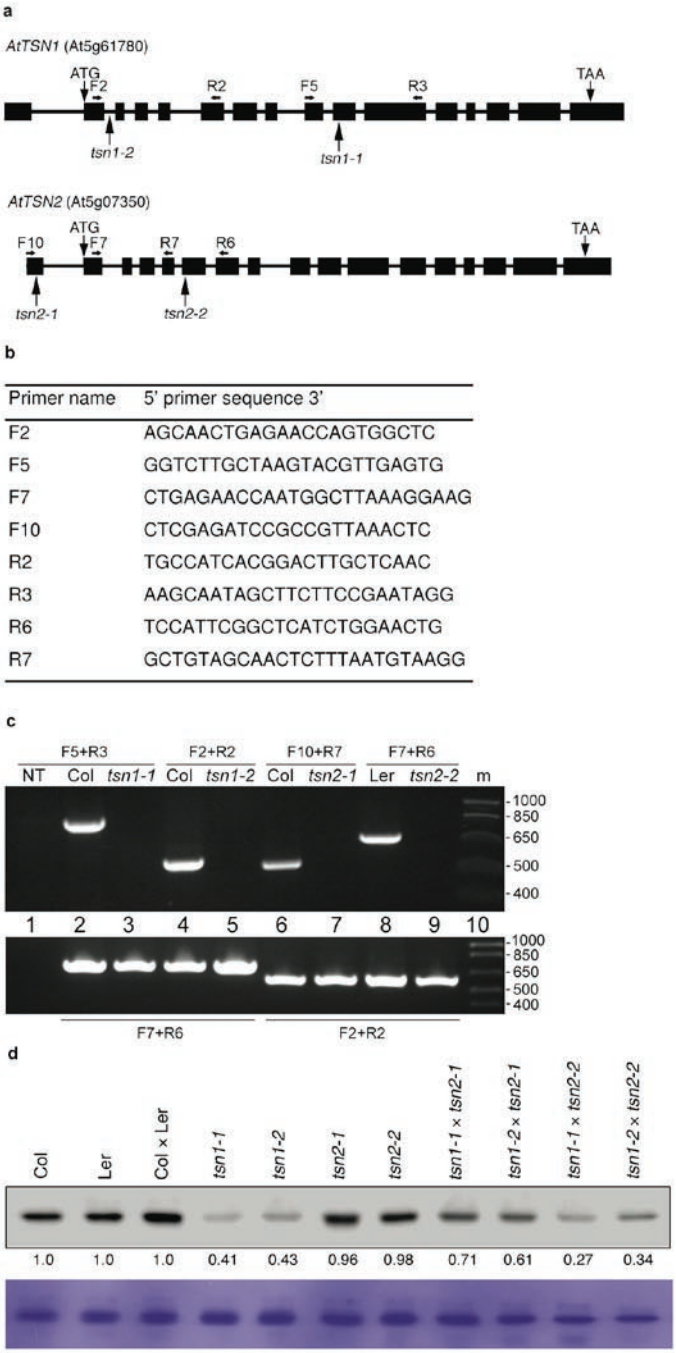

Figure S5 Characterization of the *AtTSN1* and *AtTSN2* T-DNA insertion lines. (**a**) The position of T-DNA insertions in *AtTSN1* and *AtTSN2*. Boxes and lines indicate exons and introns, respectively. The positions of primers used for genotyping are indicated by short arrows. (**b**) List of forward (indicated with F) and reverse (indicated with R) primers used for genotyping of the insertion lines. (**c**) Representative RT-PCR analysis of samples prepared from homozygous lines *tsn1-1*, *tsn1-2, tsn2-1* and *tsn2-2*, and WT (Col and Ler) plants. Lines *tsn1-1*, *tsn1-2, and tsn2-1* were generated in Col background, while line *tsn2-2* was generated in Ler backround. Amplification of the *TSN2*-specific fragment was used as control for *AtTSN1* T-DNA insertion lines and amplification of the *TSN1*-specific fragment was used as a control for *AtTSN2* T-DNA insertion lines (lower panel). The primer combinations used are indicated above and below the upper and lower panels, respectively. The nucleotide length of marker DNAs are shown on the right. NT, no template. (**d**) Western blot analysis of the total protein extracts from the wild type plants, parental insertion lines and F1 *tsn1* × *tsn2* plants using anti-TSN. Coomassie blue staining of the total protein (lower panel) was used as a loading control. Numbers shown below the upper panel correspond to the mean relative amount of TSN proteins in three independent experiments. The intensities of bands were measured by densitometry and normalized first by Coomassie blue staining and then by values of signal measured in Col, Ler or Col × Ler samples as appropriate. The amount of total TSN protein in double heterozygous plants was reduced by 30% to 70%. These results establish that simultaneous suppression of *AtTSN1* and *AtTSN2* leads to impaired plant development and low fertility. There are known examples of pronounced phenotype observed in case of double heterozygous plants, but not in case of parental homozygous lines (e.g. Siddiqui et al. 2003 Development 130, 3283; Quan et al. 2008 Plant J 53, 1013).

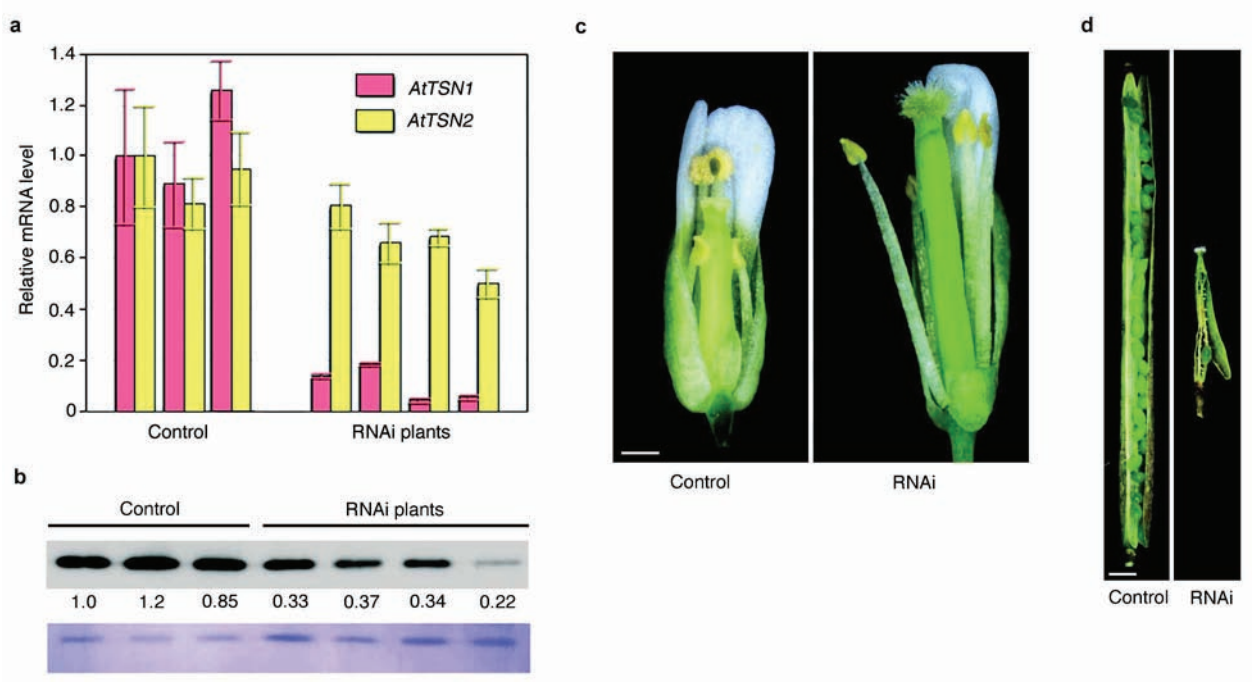

Figure S6 Down-regulation of AtTSN by RNAi causes reduction of plant fertility. (**a**) Real time quantitative PCR analysis of AtTSN1 and AtTSN2 transcript levers in three control plants transformed with empty vector and four plants transformed with vector bearing RNAi construct. The mRNA level data are presented relative to the first control plant and show mean values of three independent reactions ± s.e.m. (**b**) Western blot analysis of the total protein extracts from control and RNAi plants using anti-TSN. Coomassie blue staining of the total protein (lower panel) was used as a loading control. Numbers shown below the upper panel correspond to the mean relative amount of TSN proteins in three independent experiments. The intensities of bands were measured by densitometry and normalized first by Coomassie blue staining and then by signal measured in the sample from the first control plant. (**c**) Flower morphology in control and RNAi plants. RNAi plants produced reduced amount of pollen. Scale bar, 0.5 mm. (**d**) Siliques from RNAi plants contained very few seeds. Scale bar, 1.0 mm.

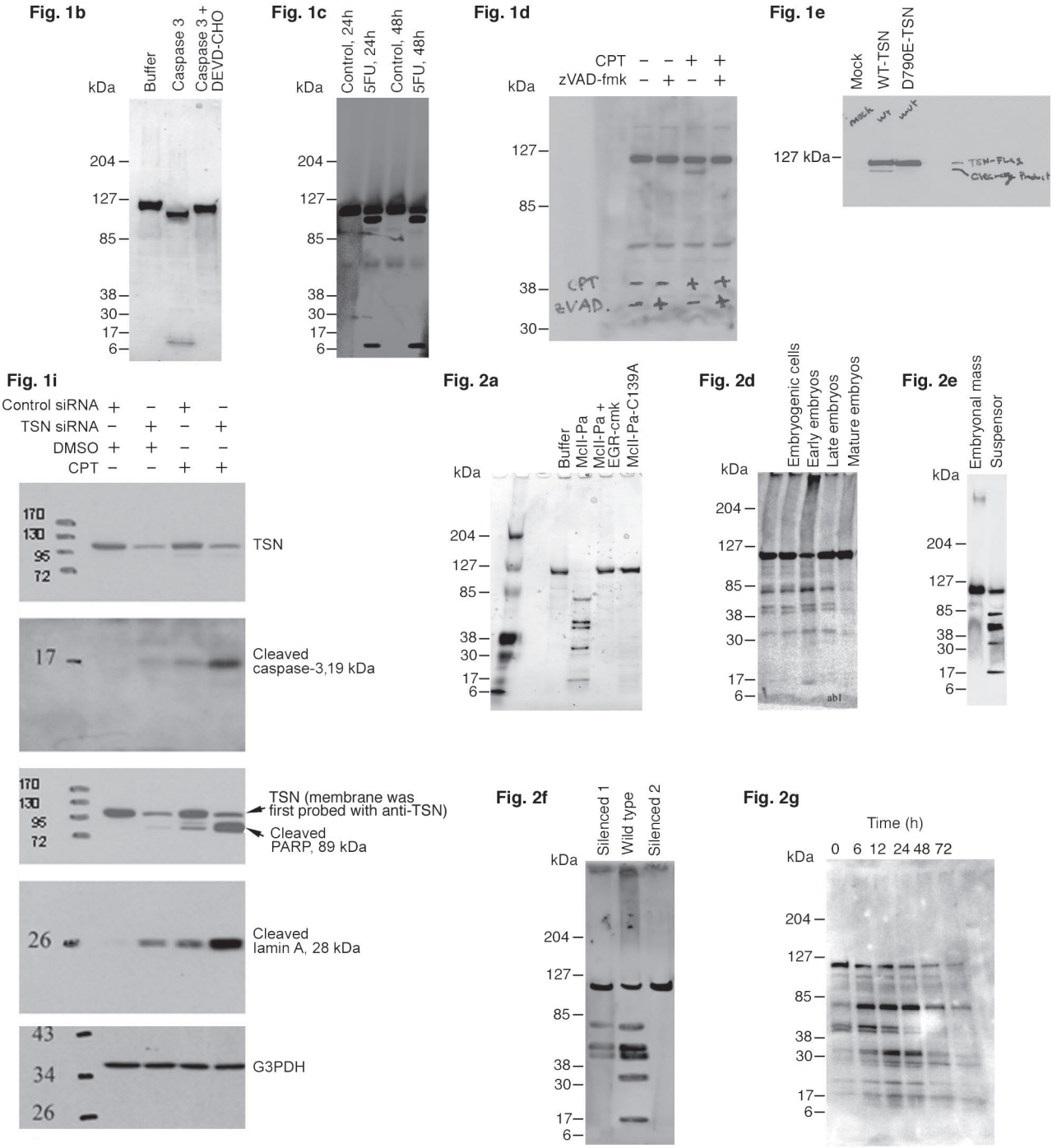

Figure S7 Full-scan or larger scan images for Fig. 1b-e, i and Fig. 2a, d-g.